

Numerical Simulation of Localized Pre flame Autoignition in Enclosures

S. M. Frolov¹, V. S. Ivanov¹, B. Basara² and M. Suffa²

¹Department of Combustion and Explosion, N. Semenov Institute of Chemical Physics

²Advanced Simulation Technologies, AVL LIST GmbH

*Corresponding author: smfrol@chph.ras.ru

A novel computational approach based on the coupled 3D Flame-Tracking – Particle (FTP) method is used for numerical simulation of confined explosions caused by pre flame autoignition. The Flame Tracking (FT) technique implies continuous tracing of the mean flame surface and application of the laminar/turbulent flame velocity concepts. The Particle method is based on the joint velocity – scalar probability density function approach for simulating reactive mixture autoignition in the pre flame zone. The coupled algorithm is supplemented with the database of tabulated laminar flame velocities as well as with reaction rates of hydrocarbon fuel oxidation in wide ranges of initial temperature, pressure, and equivalence ratio. The main advantage of the FTP method is that it covers both possible modes of premixed combustion, namely, frontal and volumetric. As examples, combustion of premixed hydrogen–air, propane–air, and *n*-heptane–air mixtures in enclosures of different geometry is considered. At certain conditions, volumetric hot spots ahead of the propagating flame are identified. These hot spots transform to localized exothermic centers giving birth to spontaneous ignition waves traversing the pre flame zone at very high apparent velocities, i.e., nearly homogeneous pre flame explosion occurs. The abrupt pressure rise results in the formation of shock waves producing high overpressure peaks after reflections from enclosure walls.

Keywords: Frontal and volumetric combustion, enclosure, numerical simulation.

1. Introduction

Numerical simulation of flame propagation with pre flame autoignition in enclosures is a complex problem. The phenomenology of the process includes flame ignition and propagation, unburned mixture compression and heating, as well as formation of hot spots and fast-spreading localized explosions in the pre flame region. The localized explosions evolve from the sites with the minimum induction time and traverse the pre flame zone as spontaneous ignition waves with the propagation velocity depending on the local instantaneous distributions of temperature and mixture composition. Better understanding of these phenomena is important for the improvement of existing measures aimed at preventing violent accidental explosions in process plants.

The objective of any combustion model in a CFD code is to provide correct values of mean reaction rates in each computational cell regardless the combustion mode (premixed, nonpremixed, partially premixed, homogeneous, inhomogeneous, spontaneous, frontal, etc.). The correct value of the mean reaction rate in the computational cell can be obtained only if one

knows the reaction kinetics and instantaneous fields of temperature and species concentrations inside the cell. The development of reaction kinetics is the separate task which is independent of the CFD combustion modeling. The only relevant issue is the CPU time required for calculating instantaneous reaction rates. This issue can be overcome by applying properly validated short overall reaction mechanisms or look-up tables.

The instantaneous fields of temperature and species concentrations inside the cell are usually not known. Therefore, one has to replace this lacking information by combustion models. There exist many combustion models both for laminar and turbulent flows. If combustion chemistry is fast as compared to mixing, the Spalding (1976) Eddy-Break-Up model can be used. It is simple but has a limited range of validity. There is a whole class of statistical combustion models (based on the formalism of probability density functions (PDF)) with probabilistic representation of turbulence and its interaction with chemistry, Pope (1990). This approach is very attractive for treating both flame propagation and autoignition problems, however requires large CPU resources. The other class of models deals with a flamelet approach, Peters (1986). In this approach, the instantaneous flame is assumed to consist of localized reactive sheets, which are transported by the flow and wrinkled by turbulent eddies. The flamelet approach is applicable when the characteristic turbulent scales are larger than a typical flame thickness. This condition is satisfied in many practical situations.

The approach supposed below is a sort of combination of flamelet and statistical combustion models to allow for simultaneous treatment of frontal combustion by explicit tracing of mean reactive surfaces and volumetric combustion by the transported PDF approach. The availability of such an approach makes it possible to attack the problem of flame propagation with preflame autoignition in enclosures.

2. Flame tracking method

The FT method deals with the subgrid model of laminar/turbulent combustion. The essence of the model can be readily explained on the example of laminar flame propagation. In the FT method, the flame surface shape and area are found based on the Huygens principle: Each elementary portion of the flame surface displaces in time due to burning of the fresh mixture at local velocity u_n (normal to the flame surface) and due to convective motion of the mixture at local velocity V . The local instantaneous velocity u_n is taken from look-up tables including in general the effects of mixture dilution with combustion products, flame stretching, and flammability limits. The local instantaneous velocity V is calculated using a high-order interpolation technique. In 2D flow approximation, the flame surface is represented by straight line segments, whereas in 3D calculations, the flame surface is represented by connected triangles.

The energy release rate in the computational cell, \dot{Q} , is composed of two terms: energy release due to frontal combustion, \dot{Q}_f , and energy release due to volumetric reactions, \dot{Q}_v . The first term \dot{Q}_f is calculated based on the estimated instantaneous flame surface area S_n , fresh mixture density ρ , and laminar flame propagation velocity u_n :

$$\dot{Q}_f = \rho Q \sum S_{ni} u_{ni} \quad (1)$$

where Q is the combustion heat and summation is made over all flame segments in the cell. The second term \dot{Q}_v is calculated using a Particle method (see below).

In the turbulent flow field, a pulsating velocity vector distorts the “mean” reactive (flame) surface by wrinkling it. The local instantaneous flame wrinkling can be taken into account by proper increasing the normal flame velocity, or in other words, by introducing a concept of local turbulent flame velocity u_t . The local turbulent flame velocity is defined as

$$u_t = u_n S / S_n$$

where S is the surface area of the wrinkled flame at a given segment, and S_n is the surface area of the equivalent “planar” flame segment.

The problem now is to find the way of calculating u_t . In the theory of turbulent combustion, there are many correlations between u_t and u_n . One of classical correlations is Shchelkin (1949) formula:

$$u_t \approx u_n \sqrt{1 + u'^2 / u_n^2} \quad (2)$$

where u' is the local turbulence intensity, related to the turbulent kinetic energy or to pulsating velocity correlations. Instead of Eq. (2) one can use other available correlations for the turbulent flame velocity.

Thus, the Huygens principle can be applied to model the “mean” shape of the turbulent flame: each elementary portion of flame surface displaces in time due to burning of the fresh mixture at local velocity u_t (normal to the flame surface) and due to convective motion of the mixture at local velocity V .

The subgrid model of turbulent premixed combustion does not differ much from that of the laminar premixed combustion, except for using u_t instead of u_n in Eq. (1). Moreover, the formulae like Eq. (2) are asymptotically valid for the subgrid model of laminar combustion (when $u' \rightarrow 0$, $u_t \rightarrow u_n$). The main problem in implementing such a combustion model into a CFD code is the development of an efficient algorithm for explicit “mean” flame-surface tracing inside computational cells. This algorithm should meet the constraints on the flame-front continuity, connectivity, etc., and the constraints on the CPU time consumption.

3. Particle method

The preflame zone exhibits volumetric reactions of fuel oxidation, formation of intermediate products like alcohols, aldehydes, peroxides, etc. In general, preflame reactions are inhomogeneous due to inhomogeneous distributions of temperature and main species concentrations and due to high sensitivity of reaction rates to these parameters. Therefore preflame reactions can result in localized energy release.

Direct (and CPU time consuming) way to calculate volumetric reaction rates is to solve the equations of chemical kinetics in the preflame zone in each computational cell. To shorten the CPU time, we introduce a certain number of notional Lagrangian particles which move in the preflame zone according to the local velocity vector. In each particle, preflame reactions proceed

at the rates determined by its instantaneous temperature and species concentrations. For determining the time and location of preflame autoignition, a certain autoignition criterion is adopted. The criterion is based on the fixed rate of temperature rise in the particle, e.g., 10^6 K/s.

The mean (over all particles in cell) reaction rate directly affects the mean flow pattern. When the autoignition criterion is met in one or several particles, new (forced) ignition sites in the preflame zone is automatically introduced. In general, these ignition sites give birth to new laminar/turbulent flame kernels or, if the preflame reactions are fast, they result in the induction (spontaneous) flames and volumetric combustion. For keeping the number of particles at a reasonable level, the consistent procedures of particle cloning and clustering are developed. The preflame particles are traced until the entire geometry is traversed by the frontal or volumetric combustion.

In each i th Lagrangian particle, the following set of equations is solved (Frolov and Ivanov (2010)):

$$\frac{dx_k^i}{dt} = u_k^i$$

$$\frac{d(\rho_l^i V^i)}{dt} = \nabla J_l^i + J_l^i \quad (3)$$

$$\rho^i \frac{du_k^i}{dt} = \frac{\partial P^i}{\partial x_k} - \nabla(Ep^i + \tau^i) \quad (4)$$

$$\rho^i \frac{dh^i}{dt} = -\nabla q^i + h_{\text{hom}}^i + \frac{\partial P^i}{\partial t} - P \frac{\partial u_k^i}{\partial x_k} \quad (5)$$

where x_k^i is the coordinate ($k = 1, 2, \text{ and } 3$) and u_k^i is the velocity component, ρ_l^i is the partial density of the l th species, ρ^i is the mean particle density, V^i is the particle volume, ∇J_l^i is the diffusion flux of the l th species to/from the particle, and J_l^i is the flux of the l th species due to chemical reaction, P^i is the mean pressure, p^i is the pulsating pressure, E is the unit tensor, and τ^i is the molecular viscous stress, h^i is the particle enthalpy, q^i is the heat flux to/from the particle, h_{hom}^i is the heat effect of chemical reaction, $\partial P^i / \partial t$ is particle heating due to adiabatic compression, and $P \partial u_k^i / \partial x_k$ is particle heating due to shock compression.

Molecular diffusion term ∇J_l^i in Eq. (3), molecular heat transfer term ∇q^i in Eq. (5) and term $\partial p^i / \partial x_k + \nabla \tau$ in Eq. (4) are modeled using classical models of Interaction by Exchange with the Mean (Pope (1985)):

$$\begin{aligned} \nabla J_l^i &= -0,5C_1(Y_l^i - \bar{Y}_l^i)\rho^i V^i \omega \\ \nabla q^i &= -0,5C_2(h^i - \bar{h}^i)\rho^i \omega \\ (\rho^i)^{-1} \nabla(p^i E - \tau^i) &= -\zeta(u_k^i - \bar{u}_k^i) + A(t) \end{aligned}$$

where C_1 and C_2 are the coefficients ($C_1 \approx C_2 \approx 2,0$), Y_l^i is the concentration of the l th species, \bar{Y}_l^i is the mean concentration of the l th species at the location of the i th particle, ω is the turbulent frequency, h^i is the enthalpy, \bar{h}^i is the mean enthalpy at the location of the i th particle, \bar{u}_k^i is the mean k th velocity component at the location of the i th particle, ζ is the coefficient ($\zeta \approx 2,075\omega$), and $A(t)$ is the stochastic function in the Langevin equation.

4. Hydrogen combustion in enclosure of complex shape

Figure 1 shows a quarter of a square enclosure with the side wall 0.2 m long initially filled with the stoichiometric hydrogen–air mixture at elevated pressure ($p_0 = 1$ MPa) and temperature ($T_0 = 850$ K). The square enclosure contains a square internal “room” 0.07x0.07 m with a “door” 0.035 m wide. The wall temperature is kept constant and equal to 293 K.

The number of flame elements per computational cell is controlled to be 10 ± 2 . The mean number of notional particles per cell is kept equal to 10 with the minimum and maximum allowable numbers of particles equal to 6 and 15. The initial flame kernel is assumed to be a circle 1 mm in radius with the center located in the symmetry center of the enclosure. Initially, the ignition kernel is assumed to be filled with combustion products at combustion temperature and $p = p_0$.

For calculating u_t , Eq. (2) is used. The laminar flame velocity entering Eq. (2) is linearly interpolated using the data of look-up tables for hydrogen. Turbulence is modeled by the standard k– ϵ model.

The rate of preflame oxidation at elevated initial pressures and temperatures is taken according to the simple relationship:

$$w = -2.25 \cdot 10^{15} p^{-1.15} [\text{H}_2]^2 [\text{O}_2] e^{-\frac{24000}{T}} \quad (\text{atm, mole, l, s})$$

This relationship is obtained by fitting the ignition delays predicted by the validated detailed reaction mechanism of Basevich et al. (2007) with that provided by the single-stage mechanism:



Figures 2a and 2b show the performance of the single-stage mechanism of Eq. (6) in terms of the comparison with the ignition delay time predicted by the reaction mechanism of Basevich et al. (2007) at $p_0 = 1$ and 4 MPa, respectively.

Note that the single-stage mechanism of Eq. (6) was used solely for reducing the CPU time. As a matter of fact, for adequate simulation of preflame autoignition a more sophisticated mechanism of hydrogen oxidation including chain-branching reactions should be used.

Two-dimensional calculations show that preflame autoignition occurs in the internal “room” and is caused by the cumulative effects of “room” corners. In addition, the availability of internal elements like internal corners and “doors” strongly affects the flow field producing additional

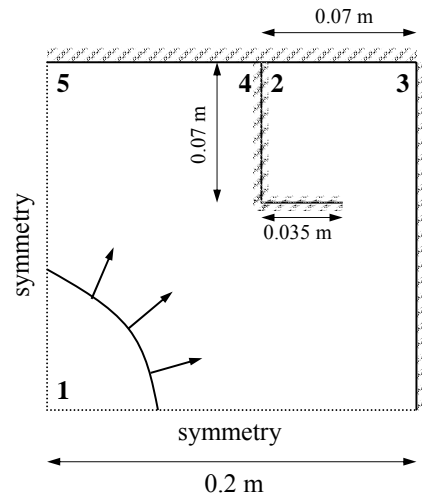


Figure 1 Computational domain for square enclosure. Points #1 to #5 denote the monitoring locations for flow parameters

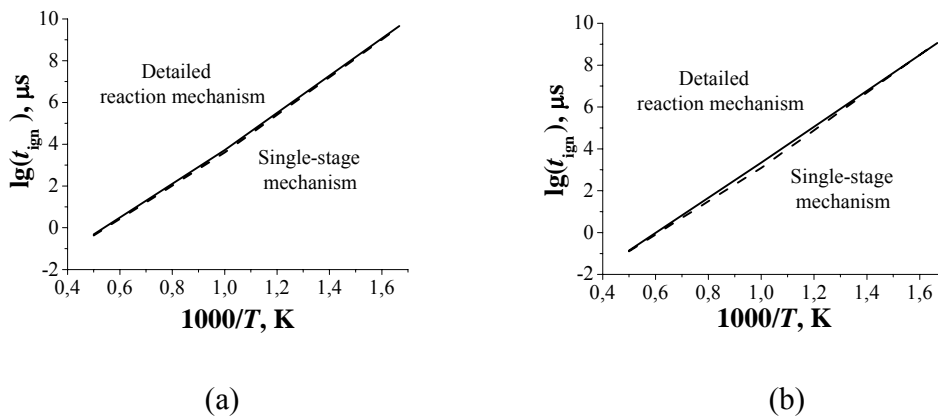


Figure 2 Ignition delay of stoichiometric hydrogen-air mixture as a function of temperature predicted by validated detailed reaction mechanism (solid curve) and single-stage mechanism of Eq. (6) (dashed curve): (a) $p = 1$ MPa, (b) $p = 4$ MPa

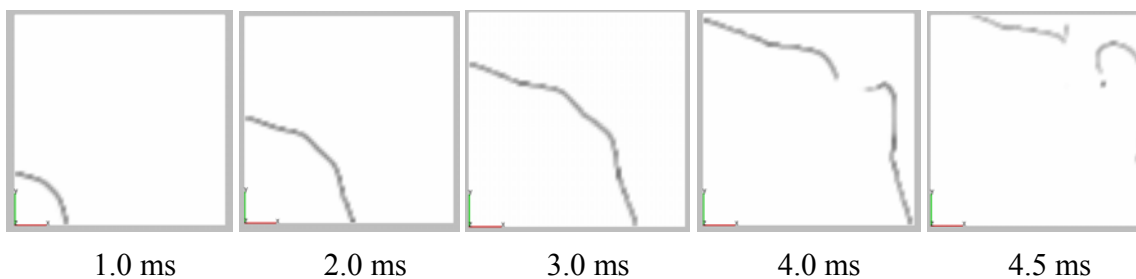


Figure 3 Snapshots of hydrogen-air flame propagation in the enclosure

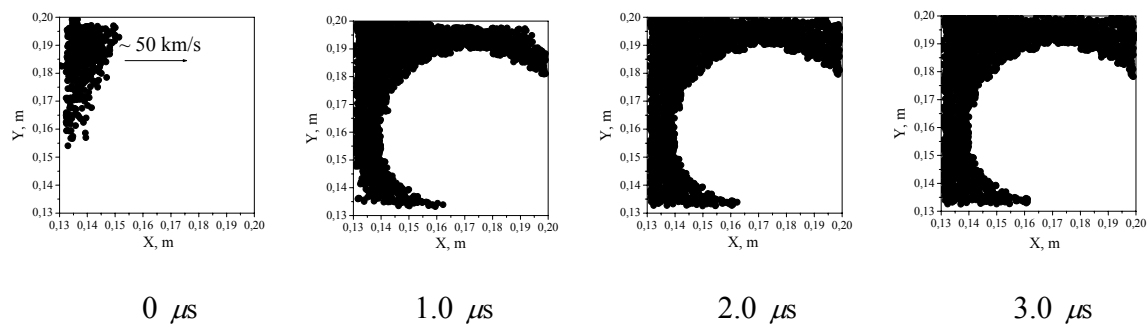


Figure 4 Snapshots of preflame autoignition in the internal “room” of the enclosure. Time intervals are counted from first autoignition events at ~ 4.85 ms

turbulence and affecting flame propagation.

Figure 3 shows the snapshots of the propagating flame. During first 3 ms the flame shape and position is insensitive to the existence of the “room”. However, when the flame reaches the external corner of the “room,” it starts to deform progressively: a flame tongue forms at the “room door” and penetrates into the “room.” The last snapshot in Fig. 3 corresponds to the time instant (4.5 ms) preceding to preflame autoignition.

Autoignition of precompressed and preheated hydrogen–air mixture ahead of the flame starts in several locations inside the “room” and spreads at the apparent velocity of ~ 50 km/s in the unburned region between flame and wall (Fig. 4). It is interesting that autoignition occurs closer to the “room” corner and walls rather than to the flame surface. This is caused by multiple reflections of pressure waves from the walls at the earlier stages of flame evolution in the enclosure and therefore more preferable conditions for mixture autoignition in the vicinity to the walls. In $1 \mu\text{s}$ after the first autoignition events, nearly all mixture in the “room” is burned except for a thin near-wall layer where the temperature is somewhat lower. The border of the white “bulb” evident in Fig. 4 at time $1 \mu\text{s}$ and later corresponds to the flame surface enveloping combustion products formed prior to preflame autoignition.

As could be expected, the autoignition pattern depends on the number of notional particles. However when the mean number of particles per computational cell is sufficiently large (on the level of 10–15 and more) this dependence becomes weak. The effect of computational grid on the autoignition pattern was also studied. The results for the grid with the mean cell size smaller by a factor of 2 were very close to those discussed herein.

The curve in Fig. 5a shows the predicted pressure history in the internal “room” corner (monitoring location #2). The predicted amplitude of the first pressure peak is about 10.4 MPa. Autoignition occurs at ~ 4.85 ms. Pressure histories in different monitoring locations are shown in Fig. 5b. The pressure wave arising due to preflame autoignition traverses the enclosure and reflects from the walls giving rise to secondary pressure peaks with the intensity considerably exceeding the maximum static pressure at normal combustion.

5. Combustion of propane in cylindrical enclosure

Figure 6 shows the vertical combustion vessel used in the experiments of Jarosinski et al. (2002). The vessel is a cylinder 172 mm in inner diameter and 360 mm high made of Plexiglas. The

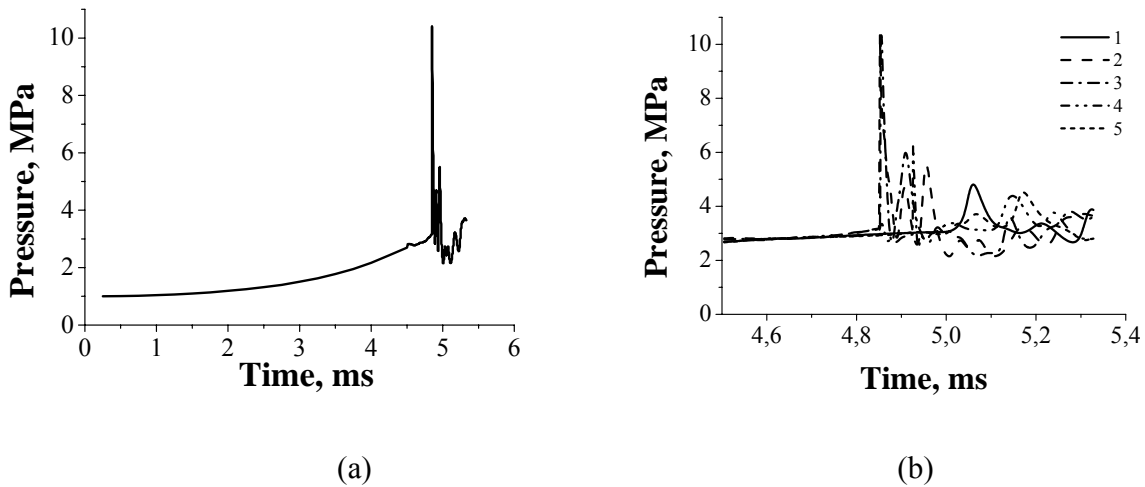


Figure 5 Predicted pressure histories in monitoring location #2 (a) and #1 to #5 (b)

vessel is fitted with an igniter at its bottom cover or in the center. The experiments were carried out with propane–air mixtures at the temperature of 293 ± 1 K. Both normal-gravity and microgravity tests were performed.

In the 3D computational example, ignition of fuel-rich propane–air mixture with equivalence ratio $\Phi = 1.1$ at normal initial conditions with normal gravity was considered. Ignition was triggered at the bottom of the vessel. All calculation settings were the same as in the example with hydrogen.

Figure 7 shows the snapshots of calculated flame front shape and position. The flame front is seen to initially elongate in vertical direction, however in the course of upward propagation it gradually flattens and becomes nearly plane at the end of the process. This behavior correlates well with experimental observations. In this example, no preflame autoignition was detected both in experiments and in calculations.

Figure 8 compares predicted and measured pressure histories in the combustion vessel for three fuel-rich propane–air mixtures. The agreement between predicted and measured results can be treated as encouraging despite combustion in experiments is seen to be less intense than in the calculations. Most probably, this effect can be attributed to heat losses to the bottom wall of the cylindrical vessel. In the present calculations we did not pay much attention to adequate modeling of heat loss. This issue will be addressed later.

In general the predicting capability of the FTP method can be treated as satisfactory. Further improvements are needed in modeling heat loss to the vessel walls as well as better modeling of the ignition stage.

6. Combustion of n-heptane in cylindrical enclosure

To show the capability of the 3D FTP method to simulate both flame propagation and preflame autoignition, we have considered the same vertical cylindrical vessel as in Section 5 but initially filled with the homogeneous stoichiometric n-heptane – air mixture at initial pressure 1 atm and elevated initial temperature 500 K. All other settings were the same as in the examples with hydrogen and propane.

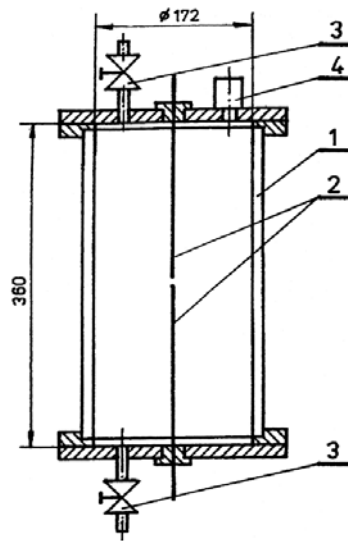


Figure 6 Combustion vessel with central ignition:
 1 – plexiglas cylinder; 2 – ignition electrodes; 3 – valve; 4 – pressure transducer

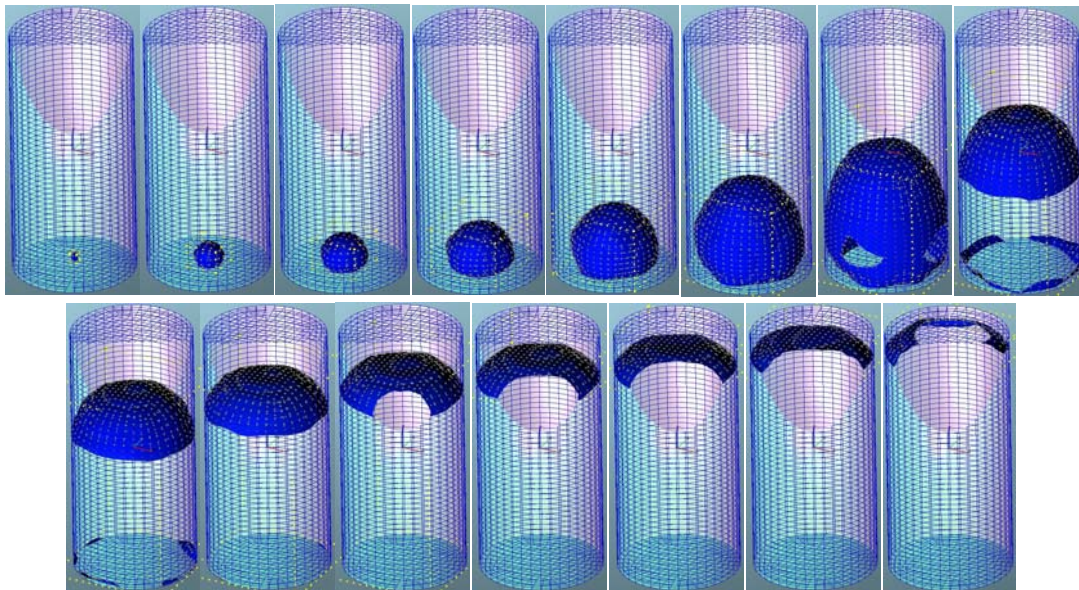


Figure 7 Snapshots of predicted flame front shape and position at different time after ignition
 (from left to right: $t = 5$ ms, 15, 25, 35, 45, 55, 65, and 75 ms)

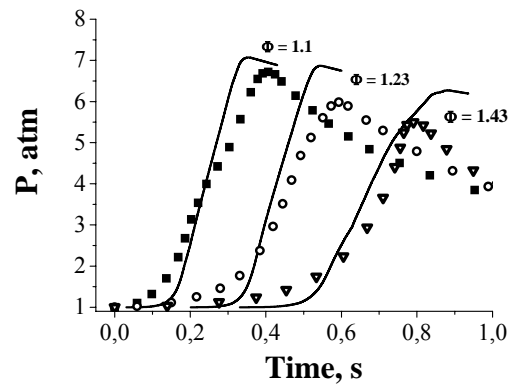


Figure 8 Comparison between predicted (curves) and measured (symbols) pressure histories

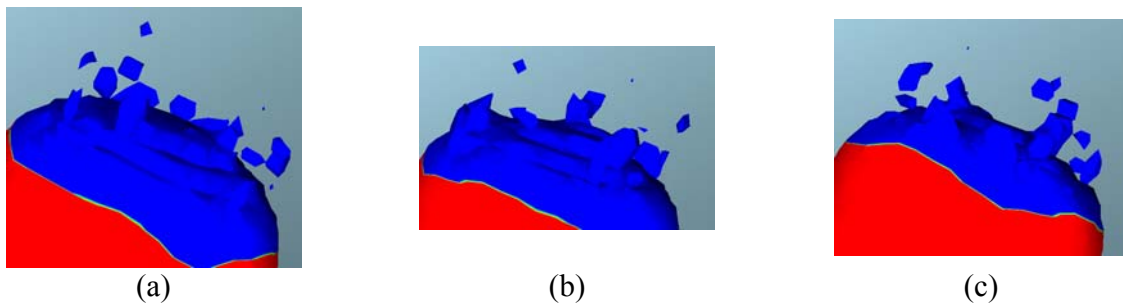


Figure 9 Predicted snapshots of preflame autoignition at ~93 ms

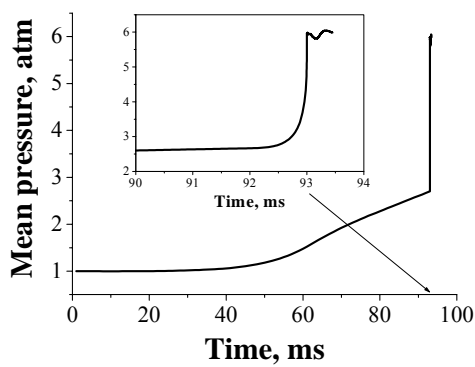


Figure 10 Predicted pressure history in the cylindrical enclosure

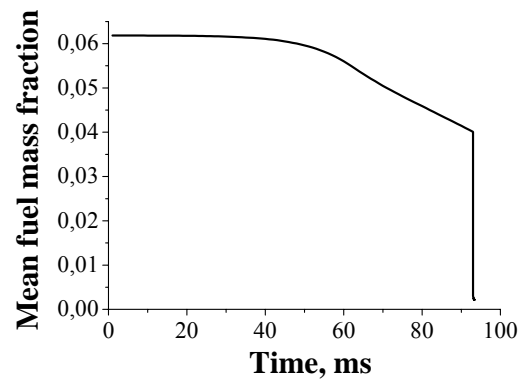


Figure 11 Predicted time history of fuel mass fraction in the cylindrical enclosure

The mixture was ignited at the symmetry axis near the bottom wall. After ignition, the flame propagated upward and the pressure in the cylinder increased. At the end of flame propagation (at time about 93 ms), preflame autoignition occurred in the upper part of the cylinder.

Figure 9 shows the results of calculations in terms of the temperature iso-surface ($T = 735$ K). One can clearly see hot spots ahead of the propagating flame. Snapshots a, b, and c correspond to the same instant of time but to different directions of view. Note that the temperature in the hot spots at this instant of time exceeds the mean preflame temperature by only about 10 K. This temperature difference arises in the course of flow evolution in the enclosure under the effect of pressure waves generated by the propagating flame and multiple pressure-wave reflections from cylinder walls.

Preflame autoignition results in the abrupt pressure rise in the preflame zone and the formation of a blast wave propagating downwards. Figure 10 shows the predicted pressure history in the vessel. Clearly, at ~93 ms there is a sharp pressure rise, followed by pressure waves in the vessel (see insert in Fig. 10). Complimentary Fig. 11 indicates that fuel in the preflame zone is depleted very quickly.

Concluding remarks

A novel computational approach based on the coupled 3D FTP method has been developed and used for numerical simulation of confined explosions with preflame autoignition. The coupled FTP method was shown to allow continuous monitoring of both flame front and preflame reactions with generation of high-intensity secondary pressure peaks.

Acknowledgments

This work was partly supported by the Russian Foundation for Basic Research (grant 08-08-00068) and AVL LIST GmbH.

References

- Basevich VYa., Frolov SM. Kinetics of 'blue' flames in the gas-phase oxidation and combustion of hydrocarbons and their derivatives. *Rus. Chem. Revs.*, 2007, 76:927.
- Frolov SM., Ivanov VS. Combined flame tracking – particle method for numerical simulation of deflagration-to-detonation transition. In: *Deflagrative and Detonative Combustion*, Ed. by G. Roy and S. Frolov. Moscow, Torus Press, 2010, pp. 133–56.
- Jarosinski J., Podfilipski J., Gorczakowski A., Veysiére B. Experimental study of flame propagation in propane–air mixture near rich flammability limits in microgravity. *Comb. Sci. Techn.*, 2002, 174:21–48.
- Peters N. Laminar flamelet concepts in turbulent combustion. *Proc. Comb. Inst.*, 1986, 21:1231–50.
- Pope SB. PDF Methods for turbulent reactive flows. *Prog. Energy Combust. Sci.* 1985, 11:119.
- Pope SB. Computation of turbulent combustion: progress and challenges. *Proc. Comb. Inst.*, 1990, 23.
- Shchelkin KI. *Fast Combustion and Spin Detonation of Gases*. Voenizd., Moscow, 1949.
- Spalding DB. Mathematical models of turbulent flames, a review. *Comb. Sci. Techn.*, 1976, 13:3–25.